Electronic Supplementary Information for:

Dipolar Repulsion in α-Halocarbonyl Compounds Revisited

Daniela Rodrigues Silva,[a,b] Lucas de Azevedo Santos,[a,b] Trevor A. Hamlin,[a] F. Matthias Bickelhaupt,*[a,c] Matheus P. Freitas,*[b] and Célia Fonseca Guerra*[a,d]

[a] Department of Theoretical Chemistry, Amsterdam Institute of Molecular and Life Sciences (AIMMS), Amsterdam Center for Multiscale Modeling (ACMM), Vrije Universiteit Amsterdam, De Boelelaan 1083, 1081 HV Amsterdam (The Netherlands)
E-mail: f.m.bickelhaupt@vu.nl, c.fonsecaguerra@vu.nl

[b] Departamento de Química, Instituto de Ciências Naturais Universidade Federal de Lavras, 37200-900, Lavras–MG (Brazil)
E-mail: matheus@ufla.br

[c] Institute for Molecules and Materials (IMM), Radboud University, Heyendaalseweg 135, 6525 AJ Nijmegen (The Netherlands)

[d] Leiden Institute of Chemistry, Gorlaeus Laboratories, Leiden University, Einsteinweg 55, 2333 CC Leiden (The Netherlands)

Table of contents

Figure S3. Energy decomposition analysis (EDA) for rigid rotation around the C–C bond as a function of the $\varphi_{O=C-C-X}$ dihedral angle of haloacetaldehydes OHC–CH_2X (X = F, Cl, Br, and I). a) rigid rotation in *syn* geometry, b) rigid rotation in *syn* geometry but with C–C distance set to 1.51 Å (as in the *syn*-iodoacetaldehyde), c) rigid rotation in *anti*-geometry, and d) rigid rotation in *anti*-geometry but with C–C distance set to 1.52 Å (as in the *anti*-fluoroacetaldehyde). Energy terms relative to the *syn* conformer, $\Delta\Delta E$, computed at ZORA-BP86-D3(BJ)/QZ4P.

Table S2. EDA terms (in kcal mol^{-1}) of the main conformations of haloacetaldehydes OHC–CH_2X (X = F, Cl, Br, and I) in the rigid rotation around the C–C bond in *syn* geometry but with C–C distance set to 1.51 Å.

Figure S4. Key closed-shell–closed-shell overlaps between fragment molecular orbitals (FMOs, isosurface at 0.03 a.u.) in the *syn* and *anti*-conformers depicted as quantitative 3D plots for the chloroacetaldehyde analogue. Analysis in rigid rotation in *syn* geometry but with C–C bond distance set to 1.51 Å, computed at ZORA-BP86-D3(BJ)/QZ4P.

Figure S5. a) Electrostatic interaction energy components, b) Pauli repulsion and key occupied–occupied orbital overlaps, and c) orbital interactions and key unoccupied–occupied orbital overlaps as a function of the $\varphi_{O=C-C-X}$ dihedral angle of haloacetaldehydes OHC–CH_2X (X = F, Cl, Br, and I). Analysis in rigid rotation in *syn* geometry but with C–C distance set to 1.51 Å. Energy terms relative to the *syn* conformer, $\Delta\Delta E$, computed at ZORA-BP86-D3(BJ)/QZ4P.

Table S3. Orbital energy gap (in eV) and overlap of key unoccupied–occupied orbital interactions of haloacetaldehydes OHC–CH_2X (X = F, Cl, Br, and I).

Figure S6. Electrostatic interaction between oxygen and halogen atoms for the C=O•••X–C colinear approach of the $OHC^{\bullet}$ and $CH_2X^{\bullet}$ fragments. a) ΔV_{elstat} as a function of the $r_{O\bullet\bullet\bullet X}$ distance (vertical lines indicate $r_{O\bullet\bullet\bullet X}$ separation in the corresponding haloacetaldehyde); b) density contours from –0.9 to 0.9 $Bohr^{-3}$ for $OHC^{\bullet}$ and $CH_2X^{\bullet}$ fragments (X = F, I for upper and lower, resp.). Computed at ZORA-BP86-D3(BJ)/QZ4P.

Figure S7. Schematic diagram of the valence configuration of the $O^{\bullet\bullet}$ and $X^{\bullet}$ (X = F and I) atoms used for the electrostatic interaction analysis shown in Figure 6c,d in the main text, in which the bare atoms approach each other along the z axis. Note that this reflects the situation for the interaction between the full $OHC^{\bullet}$ and $CH_2X^{\bullet}$ fragments, the parts of which that have been cut away, here, in the $O^{\bullet\bullet}$ and $X^{\bullet}$ systems, are shown in faded grey.

Table S4. *Syn* relative to *anti* electrostatic interaction $\Delta\Delta V_{elstat}$ energy components (in kcal mol^{-1}) of haloacetaldehydes OHC–CH_2X (X = F, Cl, Br, and I).

Table S5. Cartesian coordinates (Å), energies (kcal mol^{-1}), and the number of imaginary vibrational frequencies (N_{imag}) of the stationary points in the energy profiles for rotation around the C–C bond of haloacetaldehydes OHC–CH_2X and the open-shell $HOC^{\bullet}$ and $CH_2X^{\bullet}$ fragments (X = F, Cl, Br, and I), computed at ZORA-BP86-D3(BJ)/QZ4P.

Table S1. Homolytic bond dissociation energies (in kcal mol^{-1}) for the reaction OHC–CH_2X → OHC$^{\bullet}$ + $^{\bullet}CH_2X$ (X = F, Cl, Br, and I).

X	CCSD(T)[a]		BP86-D3(BJ)[b]	
	syn	*anti(clinal)*[c]	*syn*	*anti(clinal)*[c]
F	85.4	86.7	81.6	82.5
Cl	83.2	84.3	79.5	80.4
Br	84.3	85.8	81.2	82.6
I	86.0	88.0	81.8	83.8

[a] Computed at ZORA-CCSD(T)/ma-def2-QZVPP[1]//ZORA-BP86-D3(BJ)/QZ4P, quasi-restricted orbitals (QROs) were used for open-shell fragments; computations at *ab initio* level were carried out using ORCA[2]. [b] Computed at ZORA-BP86-D3(BJ)/QZ4P. [c] The *anti*-conformer is the global energy minimum conformation for X = F, whereas the *anticlinal* conformation is the lowest in energy for X = Cl, Br, and I.

1 (a) E. van Lenthe, R. van Leeuwen, E. J. Baerends and J. G. Snijders, *Int. J. Quantum Chem.*, 1996, **57**, 281; (b) E. van Lenthe, E. J. Baerends and J. G. Snijders, *J. Chem. Phys.*, 1994, **101**, 9783; (c) K. Raghavachari, G. W. Trucks, J. A. People and M. Head-Gordon, *Chem. Phys. Lett.*, 1989, **157**, 479; (d) D. A. Pantazis, X. Chen, C. R. Landis and F. Neese, *J. Chem. Theory*, 2008, **4**, 908. (e) J. Zheng, X. Xu and D. G. Truhlar, *Theor. Chem. Acc.*, 2011, **128**, 295.

2 F. Neese, *WIREs Comput. Mol. Sci.*, 2012, **2**, 73.

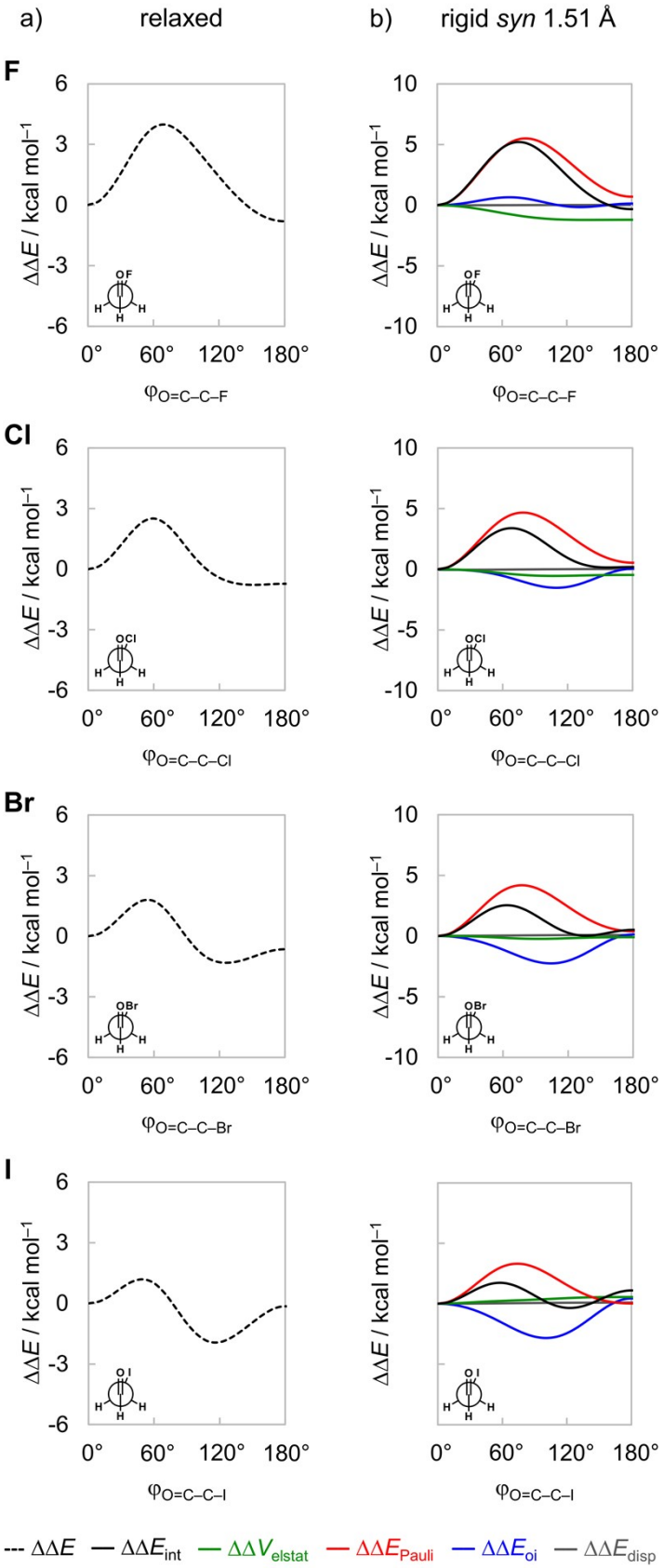

Figure S1. Rotational energy profile as a function of the $\varphi_{O=C-C-X}$ dihedral angle of haloacetaldehydes OHC–CH_2X (X = F, Cl, Br, and I). a) fully relaxed rotation around the C–C bond, and b) energy decomposition analysis (EDA) for rigid rotation in *syn* geometry but with C–C distance set to 1.51 Å. Energy terms relative to the *syn* conformer, $\Delta\Delta E$, computed at ZORA-BP86-D3(BJ)/QZ4P.

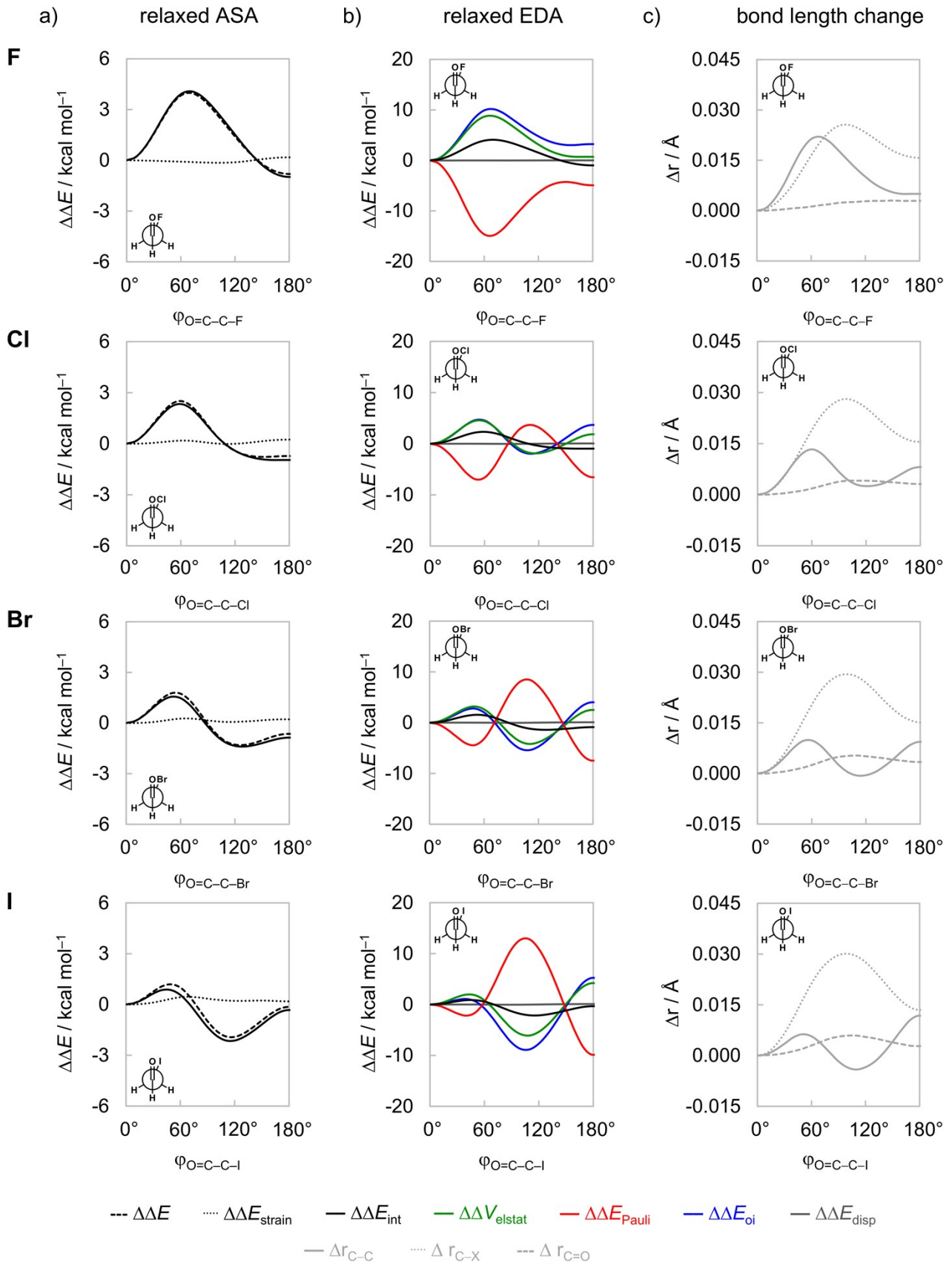

Figure S2. a) Activation strain (ASA) and b) energy decomposition analyses (EDA) of the fully relaxed rotation around the C–C bond along with c) key bond length variations as a function of the $\varphi_{O=C-C-X}$ dihedral angle of haloacetaldehydes OHC–CH_2X (X = F, Cl, Br, and I). Energy terms and distances relative to the *syn* conformer, $\Delta\Delta E$ and Δr, computed at ZORA-BP86-D3(BJ)/QZ4P.

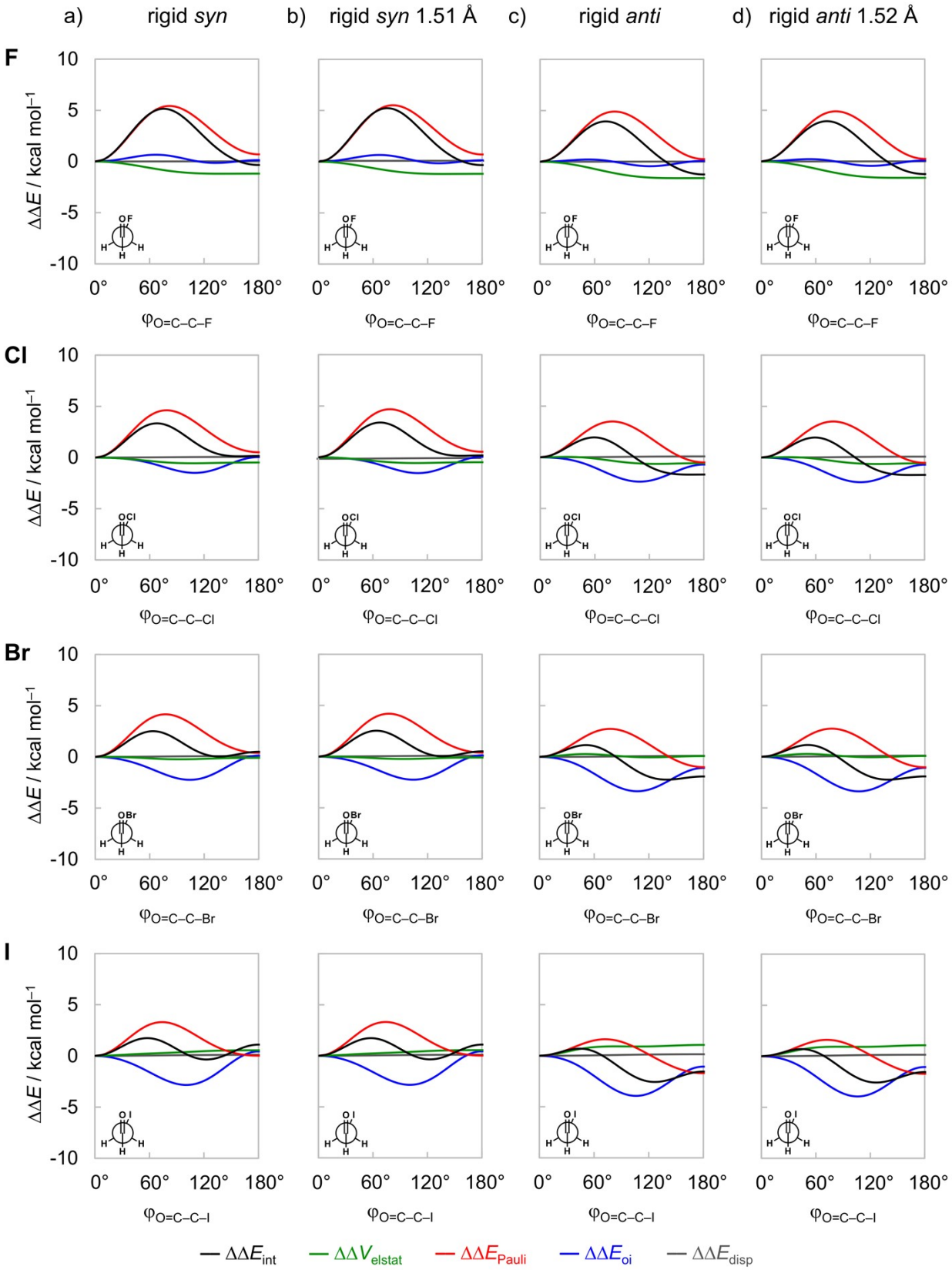

Figure S3. Energy decomposition analysis (EDA) for rigid rotation around the C–C bond as a function of the $\varphi_{O=C-C-X}$ dihedral angle of haloacetaldehydes OHC–CH_2X (X = F, Cl, Br, and I). a) rigid rotation in *syn* geometry, b) rigid rotation in *syn* geometry but with C–C distance set to 1.51 Å (as in the *syn*-iodoacetaldehyde), c) rigid rotation in *anti*-geometry, and d) rigid rotation in *anti*-geometry but with C–C distance set to 1.52 Å (as in the *anti*-fluoroacetaldehyde). Energy terms relative to the *syn* conformer, $\Delta\Delta E$, computed at ZORA-BP86-D3(BJ)/QZ4P.

Table S2. EDA terms (in kcal mol^{-1}) of the main conformations of haloacetaldehydes OHC–CH_2X (X = F, Cl, Br, and I) in the rigid rotation around the C–C bond in *syn* geometry but with C–C distance set to 1.51 Å.[a]

X	φ[b]	ΔE_{int}	ΔV_{elstat}	$\Delta V_{elstat}(n_A n_B)$[c]	$\Delta V_{elstat}(\rho_A n_B)$[c]	$\Delta V_{elstat}(n_A \rho_B)$[c]	$\Delta V_{elstat}(\rho_A \rho_B)$[c]	f[d]	ΔE_{Pauli}	ΔE_{oi}	ΔE_{disp}
F	**0**	–90.8	–181.1	36,222.3	–36,360.9	–36,304.7	36,263.2	–0.9	324.5	–232.5	–1.6
	60	–86.1	–181.8	35,711.7	–35,832.6	–35,791.5	35,731.6	–0.8	329.2	–231.9	–1.6
	120	–88.4	–182.3	35,032.5	–35,125.6	–35,102.8	35,014.5	–0.8	328.2	–232.6	–1.6
	180	–91.2	–182.3	34,813.2	–34,892.5	–34,874.5	34,772.7	–1.1	325.2	–232.4	–1.6
Cl	**0**	–90.5	–179.6	47,864.1	–48,044.2	–47,968.1	47,970.0	–1.2	327.9	–236.5	–2.3
	60	–87.2	–179.9	46,897.5	–47,041.3	–46,997.6	46,962.9	–1.3	332.1	–237.0	–2.3
	120	–89.6	–180.2	45,618.0	–45,704.6	–45,707.3	45,615.0	–1.0	330.8	–238.0	–2.3
	180	–90.3	–180.1	45,218.7	–45,276.8	–45,300.9	45,180.2	–1.2	328.5	–236.4	–2.3
Br	**0**	–91.7	–180.4	75,667.9	–75,955.0	–75,793.8	75,901.8	–1.2	330.3	–239.0	–2.6
	60	–89.2	–180.6	73,665.4	–73,875.7	–73,787.0	73,818.2	–1.4	334.0	–240.1	–2.5
	120	–91.4	–180.6	71,006.3	–71,095.1	–71,114.5	71,024.2	–1.3	332.7	–241.0	–2.5
	180	–91.2	–180.5	70,183.5	–70,212.0	–70,283.3	70,132.9	–1.5	330.7	–238.8	–2.5
I	**0**	–92.4	–181.8	100,432.6	–100,805.7	–100,584.4	100,777.3	–1.4	335.1	–242.8	–2.9
	60	–90.7	–181.5	97,469.6	–97,727.4	–97,618.0	97,696.0	–1.6	338.1	–244.4	–2.8
	120	–92.7	–181.3	93,535.1	–93,612.4	–93,672.2	93,569.6	–1.3	336.6	–245.3	–2.8
	180	–91.3	–181.2	92,318.6	–92,306.9	–92,448.7	92,257.3	–1.4	335.1	–242.4	–2.8

[a] Computed at ZORA-BP86-D3(BJ)/QZ4P. [b] The $\varphi_{O=C-C-X}$ dihedral angle (where X = F, Cl, Br, and I). [c] Sub index A for the OHC• fragment and B for the CH_2X• fragment. [d] Fitting for incompleteness of the ΔV_{elstat} term due to the use of density fitting.

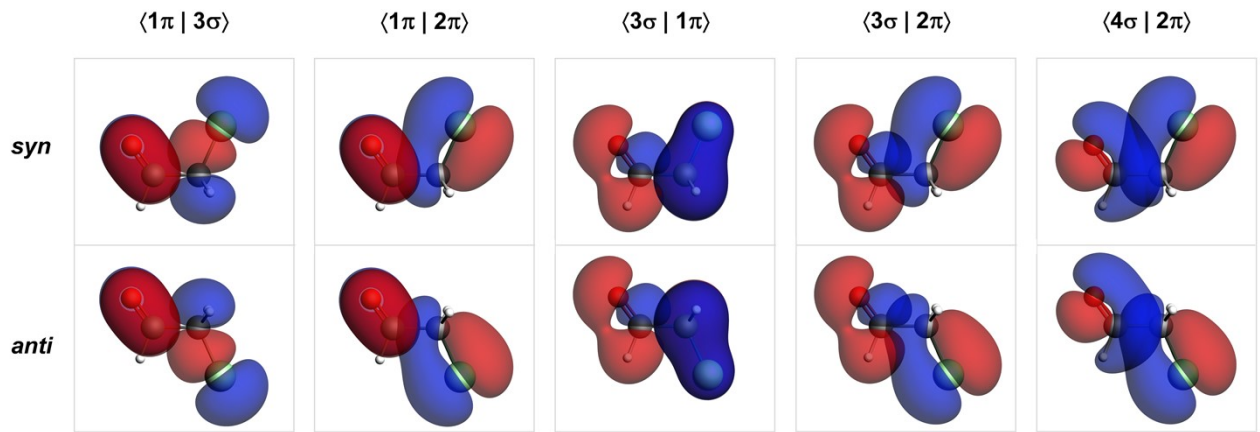

Figure S4. Key closed-shell–closed-shell overlaps between fragment molecular orbitals (FMOs, isosurface at 0.03 a.u.) in the *syn* and *anti*-conformers depicted as quantitative 3D plots for the chloroacetaldehyde analogue. Analysis in rigid rotation in *syn* geometry but with C–C bond distance set to 1.51 Å, computed at ZORA-BP86-D3(BJ)/QZ4P.

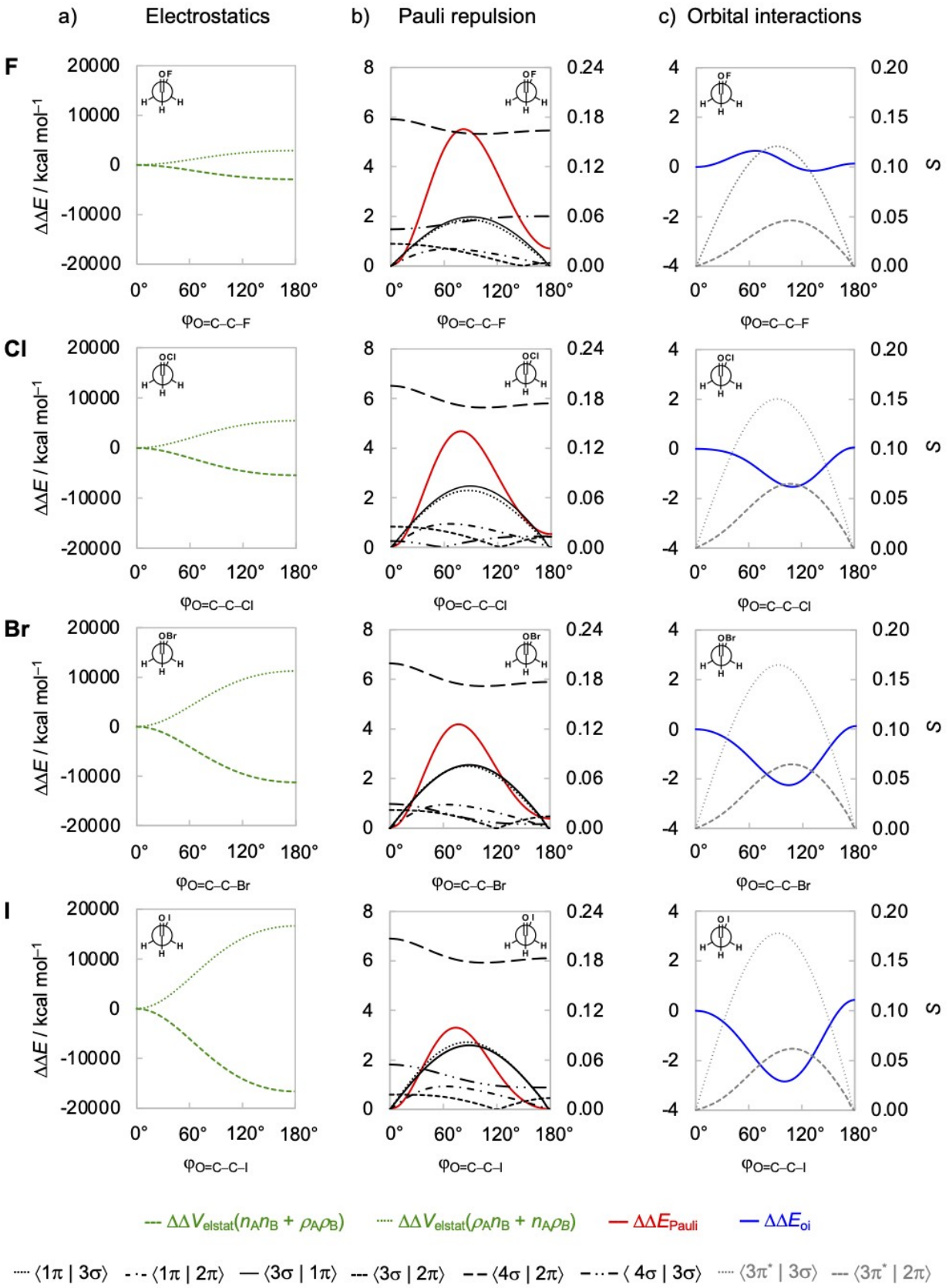

Figure S5. a) Electrostatic interaction energy components, b) Pauli repulsion and key occupied–occupied orbital overlaps, and c) orbital interactions and key unoccupied–occupied orbital overlaps as a function of the $\varphi_{O=C-C-X}$ dihedral angle of haloacetaldehydes OHC–CH_2X (X = F, Cl, Br, and I). Analysis in rigid rotation in *syn* geometry but with C–C distance set to 1.51 Å. Energy terms relative to the *syn* conformer, $\Delta\Delta E$, computed at ZORA-BP86-D3(BJ)/QZ4P.

Table S3. Orbital energy gap (in eV) and overlap of key unoccupied–occupied orbital interactions of haloacetaldehydes OHC–CH_2X (X = F, Cl, Br, and I).[a]

	$\varphi_{O=C-C-X} = 90°$ [b]			$\varphi_{O=C-C-X} = 100°$ [b]		
X	$\Delta\varepsilon_{3\pi^*-3\sigma}$ [c]	$\langle 3\pi^* \mid 3\sigma \rangle$ [c]	$S^2/\Delta\varepsilon$ x 10^3	$\Delta\varepsilon_{3\pi^*-2\pi}$ [c]	$\langle 3\pi^* \mid 2\pi \rangle$ [c]	$S^2/\Delta\varepsilon$ x 10^3
F	9.9	0.12	1.5	8.2	0.05	0.3
Cl	8.0	0.15	2.8	6.1	0.06	0.6
Br	7.3	0.16	3.5	5.4	0.06	0.7
I	6.5	0.18	5.0	4.7	0.06	0.8

[a] Computed at ZORA-BP86-D3(BJ)/QZ4P. [b] The orientation of the dihedral angle where each interaction is the most stabilizing (where X = F, Cl, Br, and I). [c] The $3\pi^*$ unoccupied orbital of the OHC• fragment and 3σ and 2π occupied orbitals of the CH_2X• fragment.

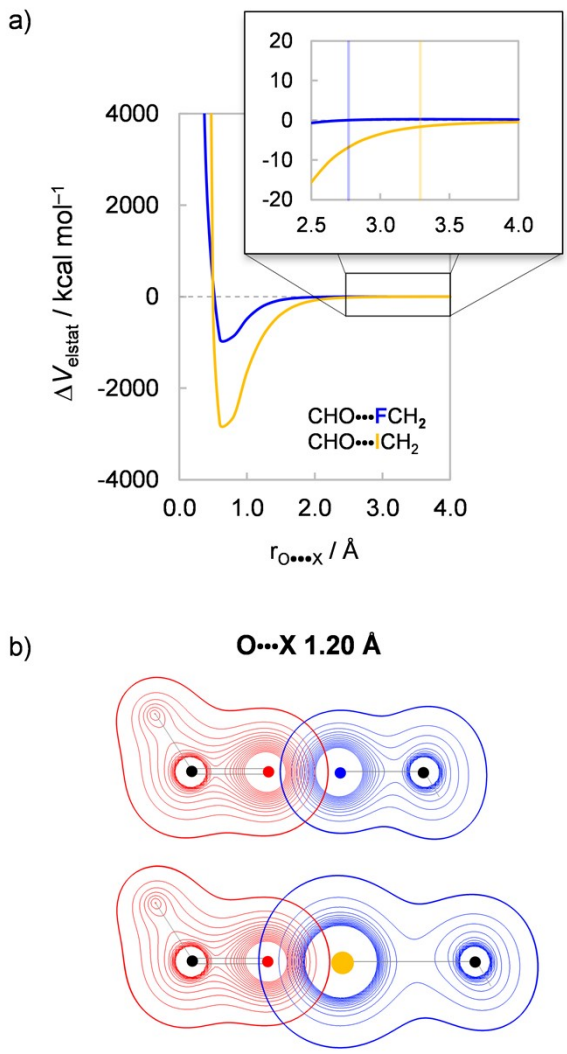

Figure S6. Electrostatic interaction between oxygen and halogen atoms for the C=O•••X–C colinear approach of the OHC• and CH_2X• fragments. a) ΔV_{elstat} as a function of the $r_{O\bullet\bullet\bullet X}$ distance (vertical lines indicate $r_{O\bullet\bullet\bullet X}$ separation in the corresponding haloacetaldehyde); b) density contours from –0.9 to 0.9 $Bohr^{-3}$ for OHC• and CH_2X• fragments (X = F, I for upper and lower, resp.). Computed at ZORA-BP86-D3(BJ)/QZ4P.

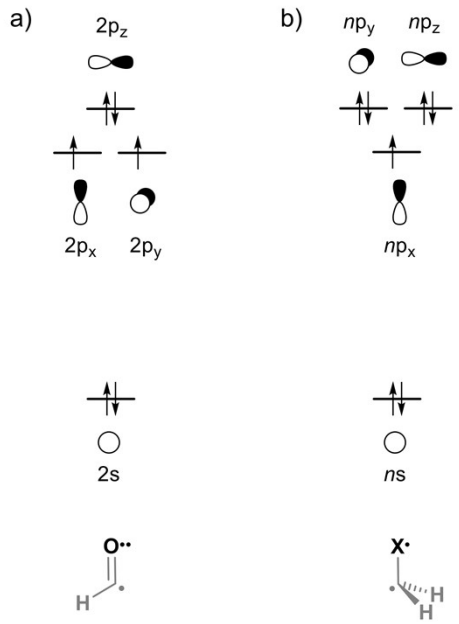

Figure S7. Schematic diagram of the valence configuration of the O•• and X• (X = F and I) atoms used for the electrostatic interaction analysis shown in Figure 6c,d in the main text, in which the bare atoms approach each other along the z axis. Note that this reflects the situation for the interaction between the full OHC• and CH_2X• fragments, the parts of which that have been cut away, here, in the O•• and X• systems, are shown in faded grey.

Table S4. *Syn* relative to *anti* electrostatic interaction $\Delta\Delta V_{elstat}$ energy components (in kcal mol^{-1}) of haloacetaldehydes OHC–CH_2X (X = F, Cl, Br, and I).[a]

X	$\Delta\Delta V_{elstat}$	$\Delta\Delta V_{elstat}$ ($n_A n_B$)	$\Delta\Delta V_{elstat}$ ($n_A \rho_B$)	$\Delta\Delta V_{elstat}$ ($\rho_A n_B$)	$\Delta\Delta V_{elstat}$ ($\rho_A \rho_B$)	Δf[b]
F	1.2	1,409.1	–1,430.2	–1,468.5	1,490.5	0.2
Cl	0.5	2,645.3	–2,667.2	–2,767.4	2,789.8	0.0
Br	0.1	5,484.4	–5,510.5	–5,743.0	5,768.9	0.3
I	–0.5	8,114.0	–8,135.8	–8,498.8	8,520.0	0.0

[a] Data from the rigid rotation in *syn* geometry but with C–C distance set to 1.51 Å, computed at ZORA-BP86-D3(BJ)/QZ4P. [b] Fitting for incompleteness.

Table S5. Cartesian coordinates (Å), energies (kcal mol^{-1}), and the number of imaginary vibrational frequencies (N_{imag}) of the stationary points in the energy profiles for rotation around the C–C bond of haloacetaldehydes OHC–CH_2X and the open-shell HOC$^{\bullet}$ and $CH_2X^{\bullet}$ fragments (X = F, Cl, Br, and I), computed at ZORA-BP86-D3(BJ)/QZ4P.

***Syn*–fluoroacetaldehyde**
E = -896.9
N_{imag} = 0

C	-0.87690441	-0.08771038	0.00000000
C	0.62587861	0.09020798	0.00000000
O	-1.45765841	-1.14626050	0.00000000
H	-1.42382489	0.89240352	0.00000000
H	0.91093353	0.67739427	0.89136772
H	0.91093353	0.67739427	-0.89136772
F	1.31416093	-1.10645390	0.00000000

***Gauche*–fluoroacetaldehyde**
E = -892.9
N_{imag} = 1, ν = -167.31607i cm^{-1}

C	-0.83525652	-0.19523154	-0.27401587
C	0.59529088	0.04530442	0.22898136
O	-1.55036127	-1.04884085	0.19663180
H	-1.18276050	0.45419916	-1.11445736
H	0.59184615	0.12021427	1.32606517
H	1.03702720	0.94626459	-0.21918065
F	1.38267224	-1.05365595	-0.13669899

***Anti*–fluoroacetaldehyde**
E = -897.8
N_{imag} = 0

C	-4.94984467	-1.64098081	-0.10863772
C	-3.50288152	-1.33117841	0.23137926
O	-5.88093173	-1.15257689	0.49082334
H	-5.08624182	-2.35646893	-0.95724304
H	-3.29567990	-1.62067126	1.27283061
H	-3.31762094	-0.25214257	0.11834504
F	-2.64062963	-2.03109418	-0.61484320

***Syn*–chloroacetaldehyde**

E = -858.5

N_{imag} = 0

C	-0.89048701	-0.08781307	0.00000000
C	0.61399877	0.08395543	0.00000000
O	-1.49392250	-1.13184604	0.00000000
H	-1.42190248	0.89958786	0.00000000
H	0.89847017	0.67147596	0.88511574
H	0.89847017	0.67147596	-0.88511574
Cl	1.53096109	-1.43954515	0.00000000

***Gauche*–chloroacetaldehyde**

E = -856.0

N_{imag} = 1, ν = -171.52758i cm^{-1}

C	-0.85977660	-0.17562469	-0.26403032
C	0.57817177	0.04991713	0.19963510
O	-1.58184633	-1.03633646	0.17886982
H	-1.21935743	0.53736243	-1.04635854
H	0.58281757	0.26623417	1.27497852
H	1.05070798	0.87011732	-0.34937489
Cl	1.57180592	-1.42502341	-0.05623762

***Anticlinal*–chloroacetaldehyde**

E = -859.4

N_{imag} = 0

C	-4.97726201	-1.74866776	0.02288883
C	-3.52267187	-1.39527007	0.28218646
O	-5.88950114	-1.06496911	0.42686150
H	-5.14357656	-2.68946686	-0.55427358
H	-3.19689745	-1.87069238	1.21740838
H	-3.40037454	-0.31141036	0.36473118
Cl	-2.46616463	-2.01151045	-1.03382574

***Anti*–chloroacetaldehyde**

E = -859.3

N_{imag} = 1, ν = -47.48150i cm^{-1}

C	-0.87006059	-0.67406376	0.00000000
C	0.47964884	0.03024507	0.00000000
O	-1.90679217	-0.05202500	0.00000000
H	-0.83574239	-1.78980380	0.00000000
H	0.56105037	0.66516679	0.89004073
H	0.56105037	0.66516679	-0.89004073
Cl	1.84763232	-1.12985756	0.00000000

***Syn*–bromoacetaldehyde**

E = -845.4

N_{imag} = 0

C	-0.89355984	-0.08655038	0.00000000
C	0.60756859	0.08151005	0.00000000
O	-1.50735768	-1.12477373	0.00000000
H	-1.42002774	0.90394928	0.00000000
H	0.90606516	0.65689473	0.88654098
H	0.90606516	0.65689473	-0.88654098
Br	1.60717417	-1.58685813	0.00000000

***Gauche*–bromoacetaldehyde**

E = -843.6

N_{imag} = 1, ν = -164.67148i cm^{-1}

C	-0.87406472	-0.15942520	-0.25271203
C	0.56684379	0.05362639	0.18322610
O	-1.59594312	-1.03134481	0.16939660
H	-1.24607057	0.58912443	-0.99588259
H	0.59856054	0.30584339	1.24940072
H	1.06008752	0.83133735	-0.40539462
Br	1.62809501	-1.58419724	-0.02182747

***Anticlinal*–bromoacetaldehyde**

E = -846.8

N_{imag} = 0

C	-4.92579432	-1.82385935	0.15807148
C	-3.47990248	-1.46180002	0.40231809
O	-5.82950487	-1.02218082	0.24362879
H	-5.10583387	-2.89097761	-0.11381579
H	-3.05882524	-2.03205314	1.23807981
H	-3.34990902	-0.38686018	0.54263845
Br	-2.45214514	-2.00321050	-1.18939026

***Anti*–bromoacetaldehyde**

E = -846.1

N_{imag} = 1, ν = -74.16080i cm^{-1}

C	-0.97388205	-0.66362509	0.00000000
C	0.40854757	-0.03197945	0.00000000
O	-1.97117871	0.02061851	0.00000000
H	-1.00996083	-1.77872742	0.00000000
H	0.53703497	0.59054340	0.89171806
H	0.53703497	0.59054340	-0.89171806
Br	1.83754363	-1.37357779	0.00000000

***Syn*–iodoacetaldehyde**

E = -834.3

N_{imag} = 0

C	-0.89843142	-0.08167042	0.00000000
C	0.60060356	0.08253120	0.00000000
O	-1.51782827	-1.11737900	0.00000000
H	-1.42552666	0.90826164	0.00000000
H	0.90487355	0.65606489	0.88531528
H	0.90487355	0.65606489	-0.88531528
I	1.70406106	-1.76113128	0.00000000

***Gauche*–iodoacetaldehyde**

E = -833.1

N_{imag} = 1, ν = -150.57024i cm^{-1}

C	-0.88838105	-0.13840872	-0.23683699
C	0.55949314	0.05895731	0.16029294
O	-1.60495475	-1.02840720	0.15751175
H	-1.28031275	0.65202063	-0.92524514
H	0.61763507	0.33910380	1.21868848
H	1.05415582	0.81513119	-0.45424644
I	1.71792178	-1.76146203	-0.01133764

***Anticlinal*–iodoacetaldehyde**

E = -836.3

N_{imag} = 0

C	-4.89438232	-1.84464147	0.20350702
C	-3.45373463	-1.48938404	0.45002462
O	-5.78258384	-1.02086707	0.15222154
H	-5.09454063	-2.93366555	0.06148973
H	-3.00589221	-2.09129461	1.24719671
H	-3.31165081	-0.41853993	0.60680989
I	-2.36120792	-2.04613549	-1.34899724

***Anti*–iodoacetaldehyde**

E = -834.5

N_{imag} = 1, ν = -103.08701i cm^{-1}

C	-1.09541926	-0.77428604	-0.13961112
C	0.23725323	-0.39169652	0.48268382
O	-2.08516465	-0.10888022	0.06203532
H	-1.11069482	-1.68662291	-0.78163092
H	0.15613277	-0.39286790	1.57457863
H	0.53327413	0.60901005	0.15134527
I	1.83494980	-1.74859412	-0.04775879

Formyl radical

E = -393.8

N_{imag} = 0

C	0.14701429	-0.33290388	0.00000000
H	0.88369536	0.52960719	0.00000000
O	-1.02716672	-0.20079752	0.00000000

Fluoromethyl radical

E = -421.4

N_{imag} = 0

H	0.07972884	0.56770797	0.96643106
C	-0.09663861	0.10262757	0.00000000
H	0.07972884	0.56770797	-0.96643106
F	-0.05927603	-1.24536088	0.00000000

Chloromethyl radical

E = -385.1

N_{imag} = 0

H	-0.06684151	0.56291984	0.95859566
C	-0.06321473	0.05778043	0.00000000
H	-0.06684151	0.56291984	-0.95859566
Cl	-0.05100973	-1.64213383	0.00000000

Bromomethyl radical

E = -370.3

N_{imag} = 0

H	-0.06707942	0.54053923	0.96024707
C	-0.06418621	0.03981111	0.00000000
H	-0.06707942	0.54053923	-0.96024707
Br	-0.04461256	-1.81882173	0.00000000

Iodomethyl radical

E = -358.7

N_{imag} = 0

H	-0.07157004	0.53622196	0.95538321
C	-0.06340755	0.02512446	0.00000000
H	-0.07157004	0.53622196	-0.95538321
I	-0.03871005	-2.02156433	0.00000000